An Enhanced Structural Damage Identification Approach Using Statistical Analysis and Optimization

Chien-Chih Kuo and Ching-Hung Lee, *Senior Member, IEEE*

***Abstract*—Structural damage identification (SDI) is of paramount importance for ensuring the long-term safety and effectiveness of various structures. However, existing identification methods require careful selection of sensors, especially in terms of sensor combination optimization, which necessitates meticulous evaluation. Herein, we propose a novel approach for detecting structural damage from vibrational signals in planar steel frames, aiming to address and improve upon the current limitations. Our method first extracts relevant vibration signals from multiple joints and then replaces the vibration signal of the damaged joint with the signal difference between the damaged and undamaged joints. This innovative approach effectively highlights the features of structural damage for further analysis. Utilizing statistical analysis, we evaluate sensor performance based on mean, standard deviation, and scatter plots, obviating the need for meticulous sensor selection. Furthermore, by analyzing the robustness exhibited by sensor combinations and confirming their stability to a certain extent, we utilize a one-dimensional fusion convolutional neural network with a signal difference (1D-FCNND) composed of individual convolutional layers using 1-D traditional and separable convolution techniques to detect structural damage accurately and efficiently. We validate the practical application of our method using benchmark data from the Qatar University Grandstand Simulator (QUGS). The results demonstrate a significant reduction in sensor requirements, accounting for only 13.33% of the total required sensors while achieving a notable enhancement of 98.92% in accuracy using only five 1D-FCNND models. The simplicity and robustness of our method enhance identification performance and optimize sensor utilization, making it a practical and promising solution for structural health monitoring (SHM) and damage identification in various engineering structures. The capability to simplify sensor selection and improve identification efficiency showcases the practical value of our method in advancing the field of SHM and damage identification.**

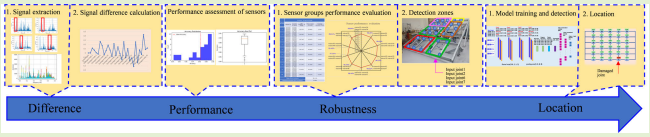

***Index Terms*— Convolutional neural network (CNN), fusion, optimization, structural damage identification (SDI).**

I. Introduction

VARIOUS damage identification methods are used in civil engineering. Song et al. [1] discussed various methods for damage identification, including model updates, genetic algorithms, neural networks, support vector machines, dynamic fingerprints, wavelet transformations, and the Hilbert–Huang transform. In [2], a method was proposed for setting a reasonable damping coefficient for damage identification in linear time-invariant structural systems. The significance of measurement signals has also been emphasized [3]. The optimization of the placement and number of sensors is vital for efficient structural damage detection.

Research on structural health monitoring (SHM) research has shown that structural damage leads to changes in the stiffness and vibrational frequency modes [4], [5]. Vibration signals are commonly measured and relevant features are extracted for analysis [6], [7]. The corresponding spectra have also been used to monitor the health of structures such as bridges to identify anomalies [8]. In [9], a statistical method was proposed to analyze the vibration data from a concrete bridge column experiencing damage. The optimization of sensor placement using an improved genetic algorithm for structures has been proposed using different methodologies [10]. However, interpretation of these results is challenging. In [11], a geometrical viewpoint parameter subset selection (GVPSS) algorithm based on the geometrical viewpoint of optimal sensor placement and a parameter subset selection method were proposed. In addition, Yi et al. [12] conducted studies and discussions on the optimal position and set a method for sensor placement. The utilization of artificial intelligence (AI) for structural damage detection through vibration

Manuscript received 30 September 2023; accepted 5 November 2023. Date of publication 14 November 2023; date of current version 14 December 2023. This work was supported in part by the National Science and Technology Council of Taiwan under Contract NSTC-111-2221-E-A49-168-MY3, Contract 110-2221-E-A49-121-MY2, Contract 110-2221-E-224-026, and Contract 110-2634-F-007-027. The associate editor coordinating the review of this article and approving it for publication was Prof. Meribout Mahmoud. *(Corresponding author: Ching-Hung Lee.)*

The authors are with the Institute of Electrical and Control Engineering, National Yang Ming Chiao Tung University, Hsinchu 30010, Taiwan (e-mail: chl@nycu.edu.tw).

Digital Object Identifier 10.1109/JSEN.2023.3330939

signals has gained interest, with convolutional neural networks (CNNs) proving effective in extracting features from large datasets. For instance, Yu et al. [13] employed CNNs to identify and locate damage in building structures, whereas Khodabandehlou et al. [14] applied a CNN for SHM on reinforced concrete bridges. However, limitations in data collection and test sizes were observed [15]. Abdeljaber et al. [15] and Abdeljaber [16] obtained joint state measurements with a 1-D CNN using the Qatar University Grandstand Simulator dataset and described the challenges of the method in handling symmetric positions. Ghazvinehwa et al. [17] selected ten joints from the same dataset, and three acceleration data points near each joint were used to train a 2-D CNN model for damage detection and localization. Teng et al. [18] trained a CNN to perform a finite element analysis and vibration experiments for steel frame damage detection. Tao et al. [19] proposed a new method for damage assessment using signal musealization and LSTM networks.

In recent years, neural networks integrated with sensor technology have been applied to various domains [20], [21], [22]. For safe driving in automated vehicles, a sensor fusion Bayesian neural network that integrates cameras, light detection and ranging (LiDAR), and radar inputs for multiobject detection was presented [20]. Chuma and Rasmussen [21] presented a metamaterial-based sensor capable of performing simultaneous microwave dielectric spectroscopy and near-infrared spectroscopy measurements for accurate substance identification. Recently, a compact-sphere airflow vector sensor using a neural network model was introduced for precise airflow measurements [22]. The sensor demonstrated high accuracy in wind speed and direction measurements in wind tunnel experiments. Ong et al. [23] introduced a 1-D deep convolution that was introduced to learn features directly from vibrational signals and to identify gear faults under different health conditions. 1D-CNN are powerful deep learning models that are widely used in data analysis, particularly for handling time-series data and 1-D signals [15], [23], [24].

Garofalo et al. [25] proposed a procedure for accurately estimating the guided wave direction in SHM using the concept of signal difference. This approach overcomes the challenges posed by the dispersive behavior of guided waves and enables precise wave direction estimation through continuous wavelet transform decomposition and cross correlation techniques with closely positioned piezoelectric transducers. In [26], a time–frequency analysis-based algorithm was proposed for locating spalling defects on switch rails using guided waves. The algorithm extracts the arrival time, frequency, and wave velocity features of the main modes of the transmission and reflection waves to predict the spalling location. In [27], the Xception architecture utilized depthwise (DW) separable convolution to replace standard convolutional layers. This study found that DW separable convolution layers outperformed traditional convolutional layers in specific image classification tasks, improving the model efficiency by reducing the number of parameters without compromising the performance. MobileNets employ DW separable convolutions to reduce the computational cost and parameters while maintaining high accuracy on devices with limited resources [28]. Howard et al. [29] extended MobileNetV3, exploring the performance of DW separable convolutions in mobile vision tasks. Liang et al. [30] introduced a deep neural network for music genre classification using DW separable convolutions to explore the application of DW separable convolutions in music genre classification.

Recently, various structural damage detection methods have been proposed. However, these methods have certain limitations. For example, the approach presented in [15] mandates the installation of sensors on all 30 joints, with each joint requiring a dedicated CNN. This results in a 100% demand rate for both sensors and models. This leads to a complex and resource-intensive configuration that poses practical challenges in real-world applications. After the initial extensive data collection, subsequent retesting becomes cost-prohibitive owing to extensive sensor deployment.

Similarly, the method described in [17] relies on the use of three adjacent sensors and individual 2D-CNNs to detect the damage in each joint. Specifically, it requires the deployment of three adjacent sensors to evaluate each joint and each joint requires a dedicated CNN, resulting in a 100% demand rate for sensors and models. This approach significantly increases the computational complexity. Furthermore, the method introduced in [31] achieves promising detection performance but exhibits a high degree of sensitivity to sensor selection, demanding meticulous adjustments based on the choice of sensors and detection region.

These limitations hold practical significance, especially in scenarios where resource constraints such as budget or spatial limitations are prevalent. In flat-plane steel facility monitoring with multiple joints, the ability to deploy a large number of sensors or perform extensive postdeployment adjustments may be limited. This underscores the need for a more practical, efficient, and robust structural damage detection method.

In response to these challenges and recognizing the practical limitations of real-world applications, our research aims to develop an innovative approach. We leverage signal processing techniques, statistical analysis, and a one-dimensional fusion CNN with signal differences (1D-FCNND) to enhance the detection performance and mitigate the impact of sensor uncertainties. In addition, we reduced the demand rate for sensors and models to 13.33%. Our goal is to provide a solution that surpasses existing methods and offers a more practical and resource-efficient alternative for structural damage detection scenarios.

The remainder of this article is organized as follows. Section II introduces the CNN architecture and QUGS dataset. Section III describes the proposed methodology and experiments. Section IV presents a verification and discussion of the results. Finally, Section V gives the conclusions.

II. CNN Architecture and QUGS Data

This section provides further insights into CNN and separable convolution, as well as the QUGS dataset, which is widely recognized as a benchmark for SHM research.

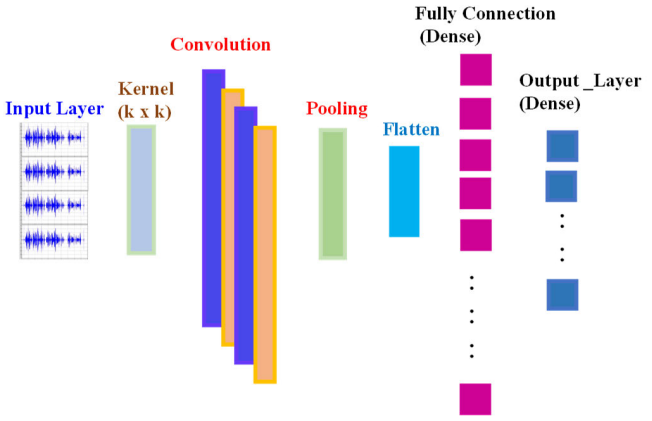

Fig. 1. CNN architecture [31], [32], [33].

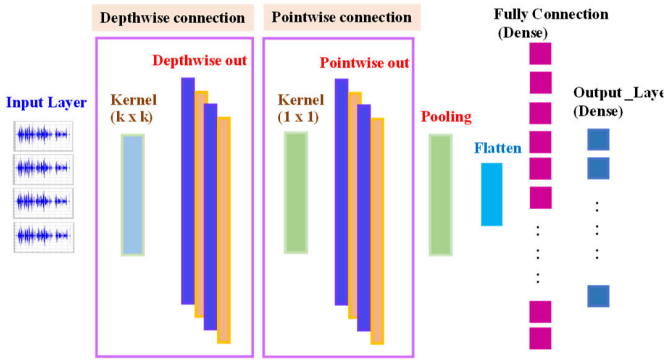

Fig. 2. Separable architecture.

A. Overview of CNN and Separable Convolution

A one-dimensional CNN (1D-CNN) is designed to extract essential local features from input data [31], [32], [33]. This is achieved by applying a small kernel that slides over the data, thereby capturing valuable patterns and information [34]. An important concept in convolution operations is parameter sharing, that is, the convolution kernel (kernel) slides on the data to capture valuable patterns and information. The process begins with the input layer, where raw data are received and prepared for the subsequent layers.

As shown in Fig. 1, our 1D-CNN architecture comprises multiple layers, each with a specific role in feature extraction and representation. The convolution layers perform the initial feature extraction, with each layer using a set of filters to detect different patterns in the data. These features are then subsampled through pooling layers, thereby reducing dimensionality and retaining critical information.

The flattened layer reshapes the output from the previous layers into a format suitable for the fully connected layers. These fully connected layers further process the learned features and enable the network to make predictions or classifications based on extracted information. In this architecture, nonlinear activation functions introduce complexities and allow the network to capture intricate relationships within the data.

Separable convolution is a specialized CNN operation that decomposes the standard convolution into two steps: DW convolution and pointwise (PW) convolution. In DW convolution, independent $k \times k$ filters are applied to process the information within each input channel without interactions between different channels. Each channel is processed individually. In contrast, the PW convolution uses a 1×1 filter to convolve the results obtained from the DW convolution. It focuses only on the data within each channel, disregarding the neighborhood information. Typically, a reduced number of filters are used during PW convolution. The advantage of using separable convolution lies in its significant reduction in computational complexity and model parameters while maintaining the model performance to some extent. This renders them suitable for resource-constrained scenarios. Separable convolution significantly reduces the computational complexity and number of model parameters while maintaining the performance of a model. The architecture of separable convolution is shown in Fig. 2.

B. QUGS Data

Qatar University (QU) has devised an innovative approach for monitoring damage in stadium structures by implementing CNN algorithms. The primary objective was to detect and identify the precise locations of damage [15]. A controlled laboratory environment was used to conduct the initial testing, employing a steel-frame simulator resembling a QU grandstand. The steel frame consisted of eight main girders and 25 filler beams. The details of the accelerometers and equipment used in the measurement setup are described in [15].

The main steel frame of the grandstand simulator was equipped with 30 accelerometers installed on the main girders at 30 joints. Specifically, 27 PCB model 393B04 accelerometers and 3 B&K model 8344 accelerometers were employed. PCB model 080A121 magnetic mounting plates were utilized to attach the accelerometers to the steel structure. In addition, a modal shaker (Model 2100E11) was employed to apply vibrations to the structure. The signal was applied to a shaker using a SmartAmp 2100E21-400 power amplifier. Two 16-channel data acquisition devices were used to generate the shaker input and collect the acceleration output.

During the experiment, a modal vibration table was employed to excite the system and record the corresponding vibrations. This facilitated the emulation of various structural damage scenarios in the experiments, with a specific emphasis on the loosening of bolts at the beam-to-beam connections. The experiments involve two critical scenarios: undamaged and damaged. In the undamaged scenario, all the bolts securing the beam-to-beam connections were fully tightened, representing a structurally intact state. In the damaged scenario, 30 bolts at different beam-to-beam connections were individually loosened to simulate structural damage. Each loosened bolt can be considered as a form of structural impairment.

The QUGS dataset utilizes a lightweight electrodynamic modal shaker capable of providing 100 pounds of peak force excitation. In addition, two piezoelectric accelerometers were employed to convert the mechanical vibrations into electrical signals to receive the vibration data. The details of the data acquisition are given as follows.

1) *Sampling Rate:* Acceleration signals were collected at a sampling frequency of 1024 Hz.
2) *Frequency Range:* Signals were collected under 0–512-Hz band-limited white-noise shaker excitation.
3) *Duration and Sample Count:* Signal recording lasted 256 s, with each signal containing 262 144 samples.
4) *Data Acquisition Software:* ME'ScopeVES was used for vibration table control and data acquisition operations.

III. Methodology and Experiments

The purpose of this study was to enhance structural damage detection using statistical analysis and sensor optimization. Our objective is to achieve overall structural damage detection using a minimal number of sensors by incorporating the concepts of input data fusion and multistage prediction. By fusing signals from the four sensors and processing ten joints for 11 classifications at each step, we performed zoned detection for the entire structure. A four-step approach is proposed to achieve the task of damage detection. Before introducing our methodology, we first explain the zone partition, utilize only ten joints, and perform 11 classifications based on the following.

1) Practical Considerations: Several fusion CNN (FCNND) partitions were utilized, each with ten joints and involving 11 classifications, where one category represents the normal vibration signal, indicating no issues in any of the joints, and the remaining ten classifications that correspond to the vibration signals of each individual damaged joint restricting each partition to 11 classifications are a reasonable and necessary choice.

2) Multistage Prediction: Our classification approach was based on the concept of multistage prediction. Due to model limitations, we divided the problem into several regional subsets, each addressing 11 classifications simultaneously. This strategy allowed us to concentrate the model's capabilities in a few categories, thereby improving the prediction accuracy.

3) Model Performance Balance: While performing only 11 classifications for each partition, our model maintained a prediction accuracy of more than 97.21%. This balance ensures model stability and performance while making a reasonable tradeoff between resource and computational costs.

4) Experimental Results and Validation: The detailed experimental results demonstrated the practical feasibility and reliability of our model, even when it was limited to 11 classifications in each zone.

First, we selected the sensor signals from joints 1, 2, 6, and 7 as inputs and considered the convenience of partitioning when choosing joints 16, 17, 21, 22, 26, and 27 for the first detection zone. We established an FCNND model, which we named FCNND1. The detection process consists of four steps. First, in the signal extraction phase, our goal is to extract the corresponding vibration signals from multiple joints. Next, we replace the vibration signals from the damaged joints with the signal difference between the damaged and undamaged joints, as shown in step A in Fig. 3. Subsequently, we conducted a performance analysis of the sensors, as shown in step B of Fig. 3. We then selected the sensor combination with the highest performance and appropriately partitioned the structure for subsequent detection, as shown in Step C in Fig. 3. Furthermore, we apply 1-D regular and separable convolution techniques to different input layers. We utilized a fusion CNN (1D-FCNND) composed of various convolutional layers to predict structural damage, as shown in step D of Fig. 3.

A. Signal Difference Analysis With Signal Extraction

1) Signal Extraction: To capture and organize the QUGS data for analysis [24], we extracted the signals received from each sensor during the simulated damage scenarios. Specifically, we compiled the vibration signals received by sensor j when joint k was undamaged/damaged, $k, j = 1, \ldots, 30$. This process enabled the assessment of the unique vibrational responses at each sensor location when specific joints were damaged. After extracting the acceleration signals of each joint, there are two sets of signals on each sensor, which were grouped together and denoted as A_j, and denoted as

$$U_j = [U_{j,k}] \tag{1}$$

$$D_j = \left[D_{j,k}\right]. \tag{2}$$

The subscript j represents the sensor number and k represents the joint number. U represents the undamaged case, denoting the signal measured on sensor j when all the other joints are undamaged. D denotes the signal measured on sensor j when sensor j is damaged only at joint j, and other joints ($j \neq k$) are damaged individually. For a combination matrix Aj of the undamaged and damaged signals on sensor j, the vibration signal is given by

$$A_j = \begin{bmatrix} U_{j,k} \\ D_{j,k} \end{bmatrix}_{j,k=1,2,\ldots,30} \tag{3}$$

and the combination of all sensors can be expressed as

$$A = \begin{bmatrix} A_1 \\ A_2 \\ A_3 \\ \vdots \\ A_{30} \end{bmatrix} = \begin{bmatrix} \begin{bmatrix} U_{1,k} \\ D_{1,k} \end{bmatrix} \\ \begin{bmatrix} U_{2,k} \\ D_{2,k} \end{bmatrix} \\ \begin{bmatrix} U_{3,k} \\ D_{3,k} \end{bmatrix} \\ \vdots \\ \begin{bmatrix} U_{30,k} \\ D_{30,k} \end{bmatrix} \end{bmatrix}_{k=1,\ldots,30}. \tag{4}$$

2) Signal Difference Calculation Method Analysis: To further optimize the sensor performance, evaluation of the signal difference selection is crucial. In this study, we employed a fusion neural network to assess five distinct signal difference methods and compared their respective performances. The structure and training details of the 1D-FCNND are introduced in step D. The results of the analysis are presented in Table I.

Table I presents a comparison of the signal difference calculation methods, along with the performance of the 1D-FCNND based on the validation accuracy and test accuracy. In the first set of experiments (ID 1), the signal differences were calculated using the "$[D_{j,k}] - [U_{2,k}]$" method, resulting in a validation accuracy of 83.96% and a test accuracy of 83.84%. Similarly, in the second (ID 2) and third (ID 3)

A. Signal difference analysis with signal extraction

1) Signal extraction

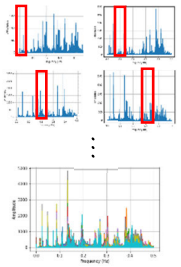

$$A = \begin{bmatrix} A_1 \\ A_2 \\ A_3 \\ \vdots \\ A_{30} \end{bmatrix} = \begin{bmatrix} \begin{bmatrix} U_{1,k} \\ D_{1,k} \end{bmatrix} \\ \begin{bmatrix} U_{2,k} \\ D_{2,k} \end{bmatrix} \\ \begin{bmatrix} U_{3,k} \\ D_{3,k} \end{bmatrix} \\ \vdots \\ \begin{bmatrix} U_{30,k} \\ D_{30,k} \end{bmatrix} \end{bmatrix}_{k=1\ldots30}$$

2) Signal difference calculation

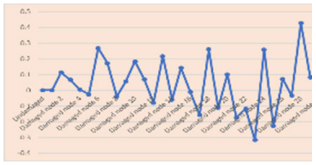

$$A_j^{diff} = \begin{bmatrix} A_1^{diff} \\ A_2^{diff} \\ A_3^{diff} \\ \vdots \\ A_{30}^{diff} \end{bmatrix} = \begin{bmatrix} \begin{bmatrix} U_{1,k} \\ D_{1,k}^{diff} \end{bmatrix} \\ \begin{bmatrix} U_{2,k} \\ D_{2,k}^{diff} \end{bmatrix} \\ \begin{bmatrix} U_{3,k} \\ D_{3,k}^{diff} \end{bmatrix} \\ \vdots \\ \begin{bmatrix} U_{30,k}^{diff} \\ D_{30,k}^{diff} \end{bmatrix} \end{bmatrix}_{k=1\ldots30}$$

B. Performance assessment of sensor-based undamaged/damaged classification using statistical analysis

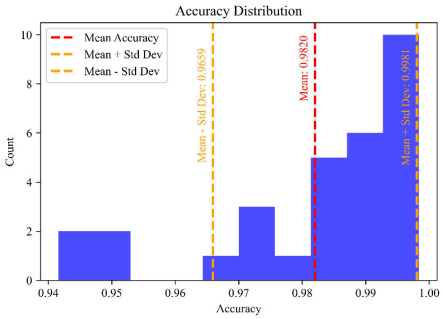

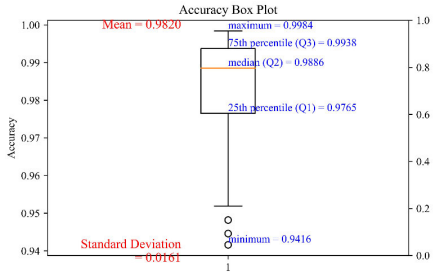

Condition of performance assessment:
1.Mean accuracy.
2.Accuracy box plot.

C. Enhancing structural damage detection through sensor groups robustness analysis and FCNN Model optimization

1) Sensor groups performance

Sensor group	Accuracy of sensors combination		
	Sensor Id	*Test accuracy of model*	*Percentage Deviation (Test)*
1	02, 04, 10, 06	98.69%	0.58%
2	02, 04, 10, 09	98.45%	0.34%
3	02, 03, 04, 10	98.61%	0.50%
4	02, 03, 10, 09	98.23%	0.12%
5	01, 02, 06, 07	98.62%	0.51%
6	02, 03, 05, 07	98.44%	0.33%
7	02, 03, 07, 08	98.20%	0.09%
8	04, 05, 09, 10	97.24%	0.90%
9	03, 04, 08, 09	96.44%	1.73%
10	01, 03, 05, 07	98.21%	0.10%
Mean (Test)			98.11%
Standard deviation (Test)			0.68%

Condition of robustness:
1.Mean accuracy.
2. Standard deviation

2) Detection zones

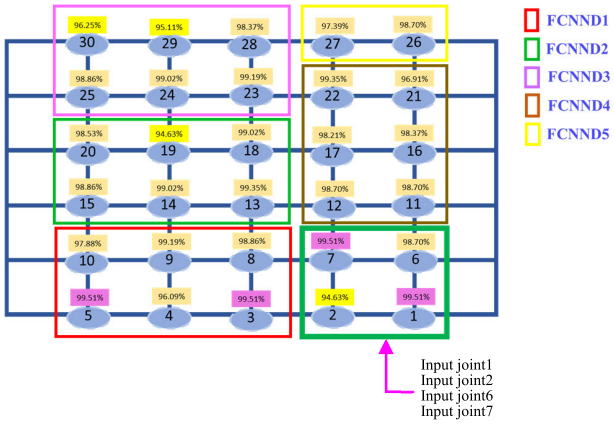

D. Model structure and damage detection

1) Model structure

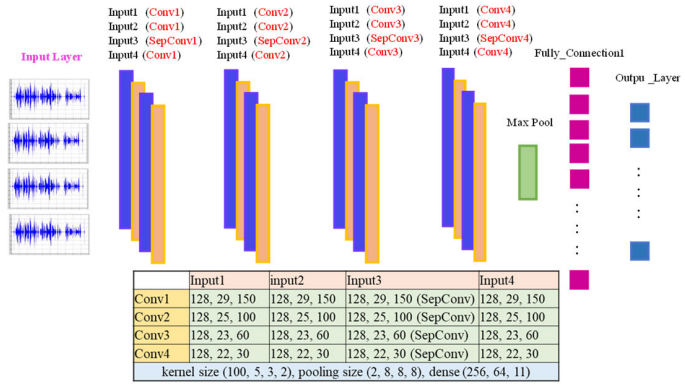

	Input1	input2	Input3	Input4
Conv1	128, 29, 150	128, 29, 150	128, 29, 150 (SepConv)	128, 29, 150
Conv2	128, 25, 100	128, 25, 100	128, 25, 100 (SepConv)	128, 25, 100
Conv3	128, 23, 60	128, 23, 60	128, 23, 60 (SepConv)	128, 23, 60
Conv4	128, 22, 30	128, 22, 30	128, 22, 30 (SepConv)	128, 22, 30
kernel size (100, 5, 3, 2), pooling size (2, 8, 8, 8), dense (256, 64, 11)				

2) Damage detection

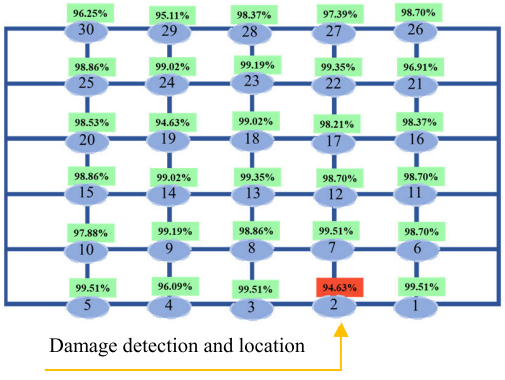

Fig. 3. Illustration flowchart of the proposed approach. (a) Signal difference analysis with signal extraction: (1) signal extraction and (2) signal difference calculation. (b) Performance assessment of sensor-based undamaged/damaged classification using statistical analysis. (c) Enhancing structural damage detection through sensor groups robustness analysis and FCNN Model optimization: (1) sensor groups performance and (2) detection zones. (d) Model structure and damage detection: (1) model structure and (2) damage detection.

TABLE I
COMPARISON OF THE SIGNAL DIFFERENCE CALCULATION METHOD

ID	Sensor signal differences	Performance (Accuracy)	
		Validation	*Test*
1	$([D_{j,k}]-[U_{2,k}])_{j,\ k=1\ldots30}$	83.96%	83.84%
2	$([D_{j,k}]-[U_{10,k}])_{j,\ k=1\ldots30}$	85.56%	85.68%
3	$([D_{j,k}]-[U_{29,k}])_{j,\ k=1\ldots30}$	84.63%	84.85%
4	$([D_{j,k}]-[U_{j,j}])_{j,\ k=1\ldots30}$	95.56%	93.87%
5	$([D_{j,k}]-[U_{j,k}])_{when\ k=j=1\ldots30}$	98.61%	98.64%

sets of experiments, we used the "$[D_{j,k}]-[U_{10,k}]$" and "$[D_{j,k}]-[U_{29,k}]$" methods, achieving validation accuracies of 85.56% and 84.63%, and test accuracies of 85.68% and 84.85%, respectively. For the fourth set of experiments (ID 4), we employed the "$[D_{j,k}]-[U_{j,j}]$" method, resulting in a validation accuracy of 95.56% and a test accuracy of 93.87%. The fifth set of experiments (ID 5) used the "$([D_{j,k}]-[U_{j,k}])_{k=j=1,\ldots,30}$" method, which yielded the highest validation accuracy of 98.61% and a test accuracy of 98.64%. The results demonstrated that the fifth experimental group (ID 5) achieved the highest damage detection accuracy, highlighting the effectiveness of this signal difference method. By focusing solely on the signal differences at the damaged joints, the model efficiently identified the features, thus enhancing detection performance.

We employed this method to calculate the signal differences for subsequent analyses. Each damaged joint is replaced by a signal difference defined as

$$D_{j,k}^{\text{diff}}=\begin{cases}([D_{j,k}]-[U_{j,k}])_{\text{when } k=j}\\ [D_{j,k}]_{\text{when } k\neq j}.\end{cases}\tag{5}$$

All the damaged signals on the sensors are replaced with signal differences, which can be represented as

$$A_j^{\text{diff}}=\begin{bmatrix}A_1^{\text{diff}}\\A_2^{\text{diff}}\\A_3^{\text{diff}}\\\vdots\\A_{30}^{\text{diff}}\end{bmatrix}=\begin{bmatrix}\begin{bmatrix}U_{1,k}\\D_{1,k}^{\text{diff}}\end{bmatrix}\\\begin{bmatrix}U_{2,k}\\D_{2,k}^{\text{diff}}\end{bmatrix}\\\begin{bmatrix}U_{3,k}\\D_{3,k}^{\text{diff}}\end{bmatrix}\\\vdots\\\begin{bmatrix}U_{30,k}\\D_{30,k}^{\text{diff}}\end{bmatrix}\end{bmatrix}_{k=1,\ldots,30}\tag{6}$$

where the superscript "diff" denotes the signal difference.

When performing the signal difference calculation, it is essential to address why the signals obtained from different time instances of the damaged experiments can be subtracted from the corresponding undamaged signals obtained at the same time. This is attributed to the fact that the undamaged condition can be achieved through a torque wrench or the use of control bolts, which is also true during actual construction. In contrast, the damage conditions of the joints exhibited more variability depending on the loosening of several bolts, which explains why the experimental results of the first three sets of signal differences were unsatisfactory.

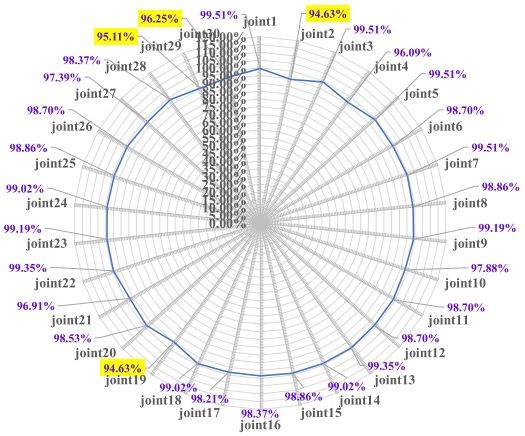

Fig. 4. Performance assessment of the sensors.

B. Performance Assessment of Sensor-Based Undamaged/Damaged Classification Using Statistical Analysis

Due to the high sensitivity of sensor signals in the working environment, it is necessary to assess the performance of these sensors. The damaged vibration signals were replaced by the signal difference, as shown in (6). We employed a 1D-CNN model for the binary classification of damaged/undamaged conditions for each joint, as shown in Fig. 4. Using commonly used statistical measures, such as the mean, standard deviation, and scatter plots, we comprehensively evaluated the performance of the sensors. The mean provides an approximate representation of the overall performance of these sensors, whereas the standard deviation indicates the extent of variation in their performance. A higher mean accuracy signifies a better overall performance, and a smaller standard deviation indicates a more stable performance. Scatter plots were employed to observe the correlation between the two variables, representing each data point as a point in a 2-D plane with one variable on the x-axis and the other on the y-axis. Scatter plots facilitated the examination of correlations, trends, and outliers. In general, when the mean accuracy exceeds 90% and the standard deviation is relatively small (less than 5%), a good and relatively stable overall performance can be considered. This indicates the usability of these sensors for identifying undamaged/damaged conditions. The detection results, shown in Fig. 5(a) as a histogram depicting the accuracy distribution and Fig. 5(b) as a box plot displaying the five summary statistics (minimum, first quartile, median, third quartile, and maximum) and potential outliers of the accuracy data, revealed a calculated mean accuracy of 98.20% and a standard deviation of 1.6%.

In Fig. 5(a), the vertical axis "count" represents the count of data points in the histogram. The box plot in Fig. 5(b) shows the data distribution and aids in identifying the outliers, as represented by the small circles in the box plot. Box plots are valuable for displaying the data range and dispersion, including values that deviate significantly from the majority

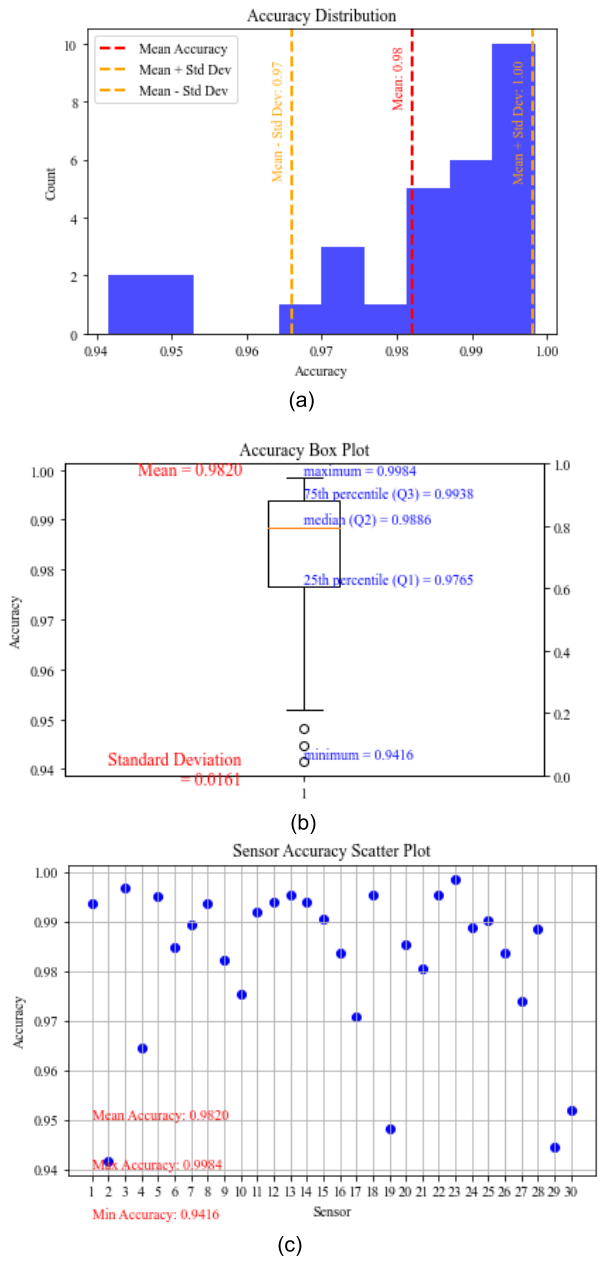

Fig. 5. Performance analysis of sensors for U/D classification. (a) Accuracy distribution. (b) Accuracy data distribution and outliers detection. (c) Scatter plot of accuracy data.

of the data. In Fig. 5(c), we observe three outliers associated with sensors 2, 19, and 29.

These outliers were deemed valid data points and were not caused by errors or measurement issues, thereby making them acceptable. Fig. 6(c) shows that the majority of the sensors exhibited higher accuracy values, with a mean accuracy approaching 98%. The highest accuracy was 99.84%, indicating the excellent performance of certain sensors in detecting structural damage. However, the lowest accuracy was 94.16%, suggesting a relatively poor performance for a few sensors. These insights allow us to understand the overall sensor performance and distribution of accuracy values. Furthermore, it helps to identify sensors that excel in damage detection and those that may require further improvement. This

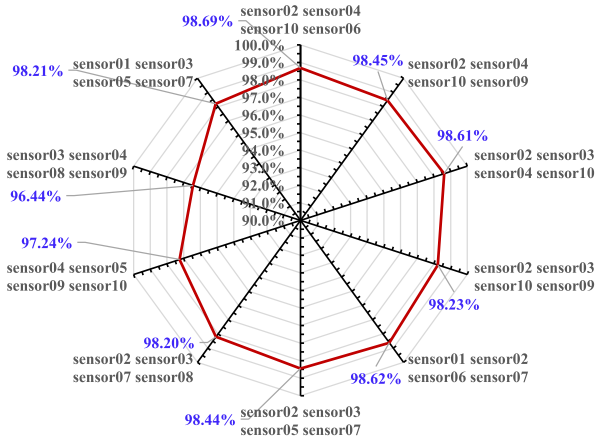

Fig. 6. Results of sensor groups' performance evaluation analysis.

chart provides valuable insights for optimizing sensor selection and enhancing the overall performance of structural damage detection systems. These findings contribute to our understanding of the sensor performance and guide improvements in detection system accuracy. This emphasizes the potential strengths and weaknesses of the sensors, enabling us to make informed decisions when selecting the most effective sensors for SHM. The information provided is crucial for enhancing the reliability and efficiency of the damage detection process, ultimately leading to safer and more efficient engineering practices.

C. Enhancing Structural Damage Detection Through Sensor Groups Robustness Analysis and FCNND Model Optimization

Appropriate sensor selection plays a critical role in achieving a comprehensive interpretation and accurate classification or prediction of outcomes using a well-trained structural damage detection model. Sensor performance and the number of sensors used are interdependent factors that must be considered. To enhance the accuracy and reliability of fault diagnosis, Jung et al. [35] proposed a sensor-selection method based on information entropy that assists engineers in selecting the most relevant sensors for fault diagnosis. This study emphasizes the importance of meticulous sensor selection. We improved structural damage detection through sensor configuration analysis and fusion strategies. First, we evaluated the performance of the sensors using a CNN model and analyzed the robustness of different sensor combinations. Subsequently, the sensor groups were combined with convenient detection zones, enabling efficient subsequent structural damage detection.

1) Sensor Group Robustness Analysis: In this study, various sensor configurations are investigated for structural damage detection. By leveraging the performance analysis presented in the preceding section, we gained valuable insights into individual sensor performance. Building on this foundation, we focused on assessing the robustness of different sensor fusion strategies concerning the predictive performance of the model.

To accomplish this, we conducted tests with the first set of sensor combinations (sensor numbers 2, 4, 6, and 10) and

TABLE II
SENSOR GROUPS PERFORMANCE EVALUATION

Sensor groups	Accuracy of sensor groups				
	Sensor Id	Accuracy of sensor	Val. accuracy of model	Test accuracy of model	Standard deviation (Test)
1	sensor02 sensor04 sensor10 sensor06	94.63% 96.09% 97.88% 98.70%	98.52%	98.69%	0.58%
2	sensor02 sensor04 sensor10 sensor09	94.63% 96.09% 97.88% 99.19%	98.28%	98.45%	0.34%
3	sensor02 sensor03 sensor04 sensor10	94.63% 99.51% 96.09% 97.88%	98.76%	98.61%	0.50%
4	sensor02 sensor03 sensor10 sensor09	94.63% 99.51% 97.88% 99.19%	97.78%	98.23%	0.12%
5	sensor01 sensor02 sensor06 sensor07	99.51% 94.63% 98.70% 99.51%	98.14%	98.62%	0.51%
6	sensor02 sensor03 sensor05 sensor07	94.63% 99.51% 99.51% 99.51%	98.67%	98.44%	0.33%
7	sensor02 sensor03 sensor07 sensor08	94.63% 99.51% 99.51% 98.86%	98.28%	98.20%	0.09%
8	sensor04 sensor05 sensor09 sensor10	96.09% 99.51% 99.19% 97.88%	97.54%	97.24%	0.90%
9	sensor03 sensor04 sensor08 sensor09	99.51% 96.09% 98.86% 99.19%	95.95%	96.44%	1.73%
10	sensor01 sensor03 sensor05 sensor07	99.51% 99.51% 99.51% 99.51%	98.25%	98.21%	0.10%
Mean accuracy (Test)				98.11%	
Standard deviation (Test)				0.68%	

utilized a fused neural network to make predictions for the first partition (indicated by the red line). The results demonstrated a remarkable damage detection accuracy of 98.69%. Subsequently, we evaluated the other combinations. The results for the first detection region (marked with a red line) are summarized in Table II, and their performances are visualized using the radar charts in Fig. 6. Fig. 6 offers a comprehensive visualization of the performance of different sensor combinations in structural damage detection experiments. The radar charts represent the predictive performance of specific sensor combinations in terms of the accuracy of structural damage detection. The radial axes in the chart represent different performance metrics. Each sensor combination exhibited a unique pattern in the radar chart, highlighting its strengths and weaknesses in detecting structural damage. The shape of the chart and area under the curve convey information regarding the balance between precision and recall, enabling us to assess the overall effectiveness of each sensor configuration.

It is evident that the sensor combinations vary in their ability to accurately detect structural damage. Most combinations performed well in terms of the performance metrics, whereas the others exhibited a more balanced overall performance. These variations in performance metrics provide valuable insights into the tradeoffs associated with different sensor configurations.

In summary, Fig. 6 serves as an important visual aid for understanding the performance differences among the different sensor combinations. This allowed us to compare their strengths and weaknesses effectively. The radar chart provides a nuanced perspective on sensor selection, resource optimization, and system robustness, offering a clearer understanding of the novel results.

In analyzing the robustness of the sensor combinations, we observed that each of the ten different sensor combinations achieved a structural damage detection performance ranging from 96.44% to 98.69% after replacing the damaged joint signal with a signal difference. The average detection performance was 98.11% with an average standard deviation of 0.68%. These results indicated minimal data deviation from the mean and low data variability across the ten test sets. Such consistent and reliable outcomes are associated with experiments or measurements that exhibit a high level of stability, in which the data points show minimal variation and are closely clustered around the mean. For the sake of structural partitioning, we selected the sensor combination in the fifth group (indicated by the thick green line) as the input to the model, which included sensors 1, 2, 6, and 7. The following observations were made.

a) Impact of sensor combination selection: Different sensor combinations exhibited only slight variations in the structural damage detection performance. This suggests that, to some extent, the choice of sensor combination does not significantly affect the performance evaluation of the detection outcome, challenging the traditional belief that selecting different combinations would substantially alter the detection performance.

b) Optimization of resource allocation: The primary rationale for exploring various sensor combinations is to optimize the resource allocation and reduce costs. Because deploying an exhaustive testing and analysis approach for each possible combination is impractical in many SHM systems that require numerous sensors, the importance of resource optimization underscores the practicality of selecting appropriate sensor combinations in real-world applications.

c) System robustness and reliability: Even with slight differences in performance (performance ranging from 96.44% to 98.69%) among different sensor combinations, the SHM system provides reliable results. This robustness is crucial for addressing sensor failures, sensor instability, and other factors encountered during practical operation.

2) Defining Detection Zones: First, we examined the performance of the sensors and found that the performance ranged from 96.44% to 98.69%, indicating a high level of sensor performance. Second, we analyzed the impact of different sensor combinations. The results showed that when signal differences were used to replace the original damaged joint signals, the choice of sensor combination did not significantly affect the detection results. All the combinations exhibited excellent predictive performance. Based on the convenience

of partitioning, we selected four input signals from sensors 1, 2, 6, and 7. We divided the detection into five zones (red, green, brown, and yellow) and trained the FCNND1–FCNND5 models. The signals used to train the FCNND1 model are denoted as $A_{1\_j}^{\text{diff}}$ as follows:

$$U_{1\_j} = [U_{1\_j,k}] \tag{7}$$

$$D_{1\_j,k}^{\text{diff}} = \begin{cases} ([D_{1\_j,k}] - [U_{1\_j,k}])_{\text{when } k=j} \\ [D_{1\_j,k}]_{\text{when } k\neq j} \end{cases} \tag{8}$$

$$A_{1\_j}^{\text{diff}} = \begin{bmatrix} U_{1\_j,k} \\ D_{1\_j,k}^{\text{diff}} \end{bmatrix}_{j=1,2,6,7,k=1,2,3,4,5,6,7,8,9,10} \tag{9}$$

where subscript 1 indicates the specific zone.

D. FCNND Model Structure and Damage Detection

This study introduces a fusion CNN (FCNND) architecture to enhance feature extraction and classification tasks. This model leverages the flexibility of the Conv1D layer by utilizing varying kernel sizes (ks) and filter quantities to capture features across different scales, thereby enhancing its expressive capacity. In addition, the introduction of SeparableConv1D layers optimizes the performance by reducing the number of parameters, making it particularly advantageous for deep networks with a large number of parameters.

1) FCNND Model Structure: A 1D-CNN extracts local features by sliding a small kernel over the data [23], [30]. Furthermore, by combining multiple convolutional and pooling layers, 1D-CNNs can be used to construct deeper models, thereby enhancing the learning capabilities. To further enhance the performance and efficiency of our model, we introduced the concept of FCNND. This differs from the approach used in [36], in which a classifier is employed as the fusion mechanism to receive the raw output signals and combine the predictions of multiple models or classifiers. However, using a classifier as a fusion mechanism can lead to suboptimal results or overfitting if the models are similar or use similar feature sources.

In contrast, our FCNND approach utilizes different types of convolutional kernels at the input layer, including standard and separable convolutions, to increase the model's perception of diverse features. The main distinction between these two methods is their fusion strategy. In this study, we combined two different types of convolutions at the input layer: standard convolution, where the same kernel is applied to each input channel (convolving across all input features), and separable convolution, where each input channel uses a different kernel (performing depth-wise convolution followed by point-wise convolution). By integrating these two types of convolutions, the FCNND effectively harnesses their respective advantages. Standard convolution captures comprehensive features, whereas separable convolution significantly reduces computational resources.

The ultimate goal of FCNND is to maintain the model performance while minimizing the number of parameters and computational costs, making the method scalable and widely applicable. In addition, we conducted a detailed investigation of the timing of introducing separable convolutional layers, as shown in Table III.

TABLE III
COMPARISON OF CONVOLUTION CONFIGURATIONS AND PREDICTION PERFORMANCE IN FOUR TEST SCENARIOS

Model	Input Layer Convolution				Prediction Perf.	Total Params	Feat. Count
	Layer 1	*Layer 2*	*Layer 3*	*Layer 4*	*Test Accuracy*		
1	SepConv	Conv	Conv	Conv	96.51%	1,053,628	1360
2	Conv	SepConv	Conv	Conv	95.96%	1,053,628	1360
3	Conv	Conv	SepConv	Conv	98.20%	1,053,628	1360
4	Conv	Conv	Conv	SepConv	98.14%	1,053,628	1360
5	Conv	Conv	Conv	Conv	98.12%	1,141,008	1360

2) Model Comparison and Performance Evaluation: Table III presents the experimental results in which we compare the performances of five distinct models (models 1–5) across five different testing scenarios. Models 1–4 employ 1D-FCNND, a fusion of standard and separable convolution techniques, whereas model 5 utilizes 1D-CNN, omitting the use of separable convolutions.

Model 1 employs separable convolutions applied individually to the first input data. Separable convolutions are a specific type of convolution operation within neural networks that are renowned for their separation of spatial convolutions within channels and DW convolutions across channels. In this scenario, model 1 employs separable convolutions to process the first input. Model 2 applies separable convolutions to the second set of input data. Model 3 applies these to the third input dataset. Model 4, similar to the preceding models, employs separable convolutions but applies them to the fourth input data. The key distinction of model 5 is the omission of separable convolutions instead of utilizing a traditional 1D-CNN.

The performance of these models was assessed across five distinct testing scenarios, demonstrating variations in their performance under different conditions. The purpose of this table is to investigate the influence of different convolution configurations on the predictive performance, facilitating a better understanding of the importance of selecting suitable convolutional models for various tasks and datasets.

Model 3 achieved the highest accuracy (98.20%) with a reduced number of parameters (1 053 628) due to the use of DW separable convolutions. In contrast, model 5 employed regular convolutions throughout (1 141 008 parameters) and achieved an accuracy of 98.12%. In this section, we discuss their performance and generalization capabilities. Model 3 demonstrated superior performance in capturing essential features during the training process, resulting in optimal predictive outcomes. Furthermore, it exhibits better generalization capabilities when dealing with previously unseen data, making it a more robust and versatile model. In contrast, model 5 encountered overfitting.

It is essential to recognize that the performance of a model is not solely determined by the number of parameters. Instead,

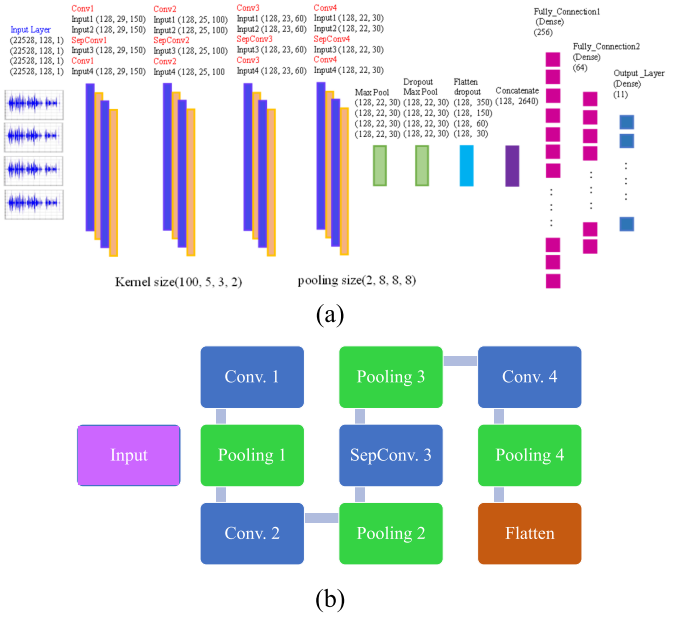

Fig. 7. Fusion CNN model structure. (a) FCNND model. (b) Convolution process.

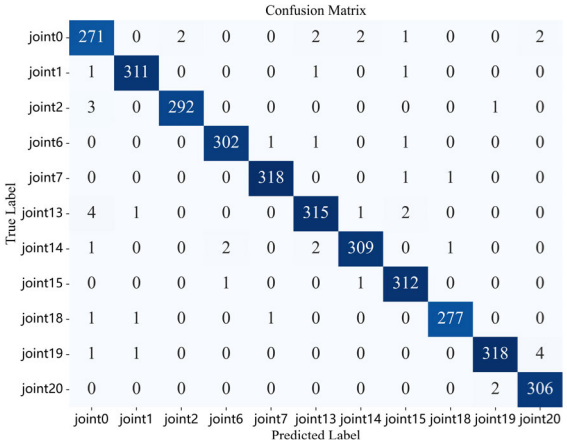

Fig. 8. Confusion matrix.

it is a performance evaluation based on various factors, including the number of features, model architecture, and training methodology. Therefore, when selecting a model, it is crucial to comprehensively consider these factors to identify the most suitable. In this study, model 3 demonstrated better predictive performance with a reduced number of parameters than the other models.

Our proposed model aims to efficiently extract pertinent features from sensor data while optimizing the sensor placement to enhance the accuracy of structural damage detection. The network architecture for this approach is visually shown in Fig. 7(a) and (b). In the following, we explain the model construction process and role of each layer.

The proposed model architecture encompasses four distinct input layers, each embedding a sequence of convolutional and pooling layers to form a multitiered feature extraction system.

Each input layer is configured with a distinct convolutional layer setup to cater to varying levels of feature learning demands. Within these input layers, particularly in the third and remaining input layers, we introduce different types of convolutional layers, including separable and standard convolutional layers. This design strategy enables the model to capture diverse feature types at multiple levels.

For the separable convolutional layer, we employed a specialized convolutional operation in the third input layer. The separable convolutional layers achieve convolution by decomposing the operation into two independent stages: DW and PW. The DW convolution handles the spatial relationships among different channels within the input data, whereas the PW convolution conducts convolutions independently across channels. This decomposition structure not only effectively reduced the number of model parameters, thus mitigating the risk of overfitting, but also accelerated the training process.

Simultaneously, standard convolutional layers were applied to the first, second, and fourth input layers. Standard convolutional layers represent the classical convolution operation, which extracts features by sliding convolutional kernels over the input data. These convolutional layers capture both local and global features within the input data and are capable of learning diverse feature representations during the training process. By utilizing standard convolutional layers across multiple input layers, we further enhance the ability of the model to grasp feature abstractions at various levels.

In summary, our model strongly emphasizes multitiered feature extraction and fusion through its architecture. By incorporating different types of convolutional layers, including separable and standard convolutional layers, the model becomes proficient at learning diverse feature representations across multiple abstraction levels. Consequently, it demonstrates remarkable performance across various scenarios.

For the filter selection process, we provide the following explanations.

a) Feature hierarchy: Our choice of convolutional ks allowed the capture of features at different hierarchical levels within a signal. We employed larger ks, such as 100, to capture global signal features, whereas smaller kernels (e.g., two or three) were utilized to focus on finer local details. This approach allowed our model to address both the overall signal structure and intricate local features simultaneously. As indicated by the confusion matrix, we achieved a favorable predictive performance (see Fig. 8).

b) Multiscale analysis: By incorporating convolutional kernels of diverse sizes, our model can analyze signals at multiple scales. This enhances the model's understanding of signal content and its adaptability to variations in object size and shape.

c) Hyperparameter optimization: The convolutional ks is considered a hyperparameter that requires tuning. Through experimentation with various ks, we identified the optimal sizes tailored to a specific task. The final selection of these sizes was based on empirical results, providing robust support for our choice.

d) Overfitting mitigation: Relying solely on large convolutional kernels could potentially lead to overfitting because the model might memorize a greater number of training samples. The incorporation of convolutional kernels of varying sizes

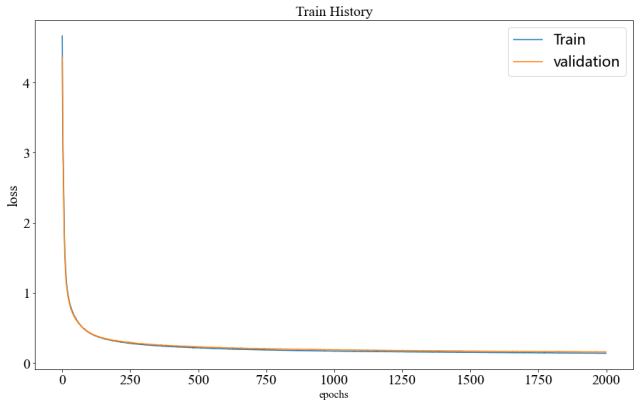

Fig. 9. Loss during model training.

TABLE IV
PERFORMANCE COMPARISON OF FUSION CNNS ON FIVE ZONES FOR DETECTION

ID of sensors	FCNND Zone	Performance of FCNND	
		Val. accuracy	*Test accuracy*
1,2,6,7,3,4,5,8,9,10	FCNND1	98.61%	98.64%
1,2,6,7,13,14,15,18,19,20	FCNND2	98.73%	98.92%
1,2,6,7,23,24,25,28,29,30	FCNND3	92.63%	93.81%
1,2,6,7,11,12,16,17,21,22	FCNND4	97.66%	98.20%
1,2,6,7,26,27	FCNND5	98.14%	98.62%

serves as a regularization technique that reduces the risk of overfitting (as shown in Fig. 9). This is because the model requires diverse scale information for accurate predictions.

Table IV presents the experimental results, which show that utilizing signal differences enhances the robustness of the system. In the presence of various uncertainties, anomalies, or external interferences, the system can maintain stable performance and functionality, rendering it reliable for damage detection. We further examined the third group from Table IV, which exhibited a relatively low prediction performance (still achieving an accuracy of 93.81%).

3) Analysis of Factors Contributing to Model Performance: Model 3 achieved the highest accuracy (98.20%) with a reduced number of parameters (1 053 628) due to the use of DW separable convolutions. This exceptional performance can be attributed to the ability of separable DW convolutions to efficiently capture spatial relationships within the input data. The separable convolution operation effectively decomposes the convolution into depth- and point-wise convolutions, thereby reducing redundancy and promoting feature learning. This not only led to superior feature extraction but also contributed to mitigating the risk of overfitting.

In contrast, model 5, which relied on regular convolutions, exhibited a slightly lower accuracy of 98.12%. This result emphasizes the importance of selecting suitable convolutional configurations for the tasks. The overfitting issue observed in model 5 underscores the advantages of our FCNND architecture, which carefully balances model complexity and performance. The flexibility of our architecture in utilizing varying ks and filter quantities allowed it to capture features across different scales, thereby enhancing the expressive capacity of the model.

Furthermore, the choice of convolutional layers at the input level plays a crucial role in the performance of the proposed model. By incorporating standard convolution, which applies the same kernel to all input channels, and separable convolution, which uses different kernels for each channel, our FCNND effectively harnesses its respective advantages. This diversity in the convolution types contributes to the ability of the model to capture diverse features across multiple abstraction levels.

These results highlight the significance of our FCNND architecture, which not only achieves high accuracy but also offers insights into the importance of convolutional configurations in structural damage detection. The superior performance of model 3 can be attributed to its efficient feature extraction, parameter reduction, and thoughtful convolutional layer selection, which, when combined, form the core reason for its exceptional results.

Now, we shall provide a detailed explanation of the attributes of our method, which is referred to as the fusion CNN (FCNND), and how they differ from those of the traditional 1D-CNN method.

4) Key Highlights and Distinctions:

a) Flexibility of multiple convolutional kernels: FCNND uses Conv1D layers with varying ks and filter quantities, thereby enhancing its ability to capture features at different scales. This flexibility enables the proposed method to effectively handle multiscale structural features.

b) Introduction of separable convolutions: We introduce separable convolutional layers to optimize performance while reducing the overall number of parameters (as indicated in Table III). This optimization is particularly advantageous for deep networks with substantial parameter counts, enhancing both the efficiency and scalability for practical applications.

c) Divergent fusion strategy: In contrast to the 1D-CNN approach (as demonstrated by model 5 in Table III), our fusion strategy (FCNND) leverages different types of convolutions, including standard and separable convolutions, at the input layer. This enhances the model's ability to perceive diverse features. Our method emphasizes divergence in the fusion strategy and demonstrates the effectiveness of this approach.

d) Balance between performance and parameters: By conducting performance comparisons among different models, we comprehensively consider factors such as the number of parameters, model architecture, and training methods. This aids in selecting the most suitable model for a specific task. In our study, model 3 exhibited outstanding performance with fewer parameters, making it a high-performance, resource-efficient choice.

In summary, our approach offers several key distinctions, including flexible convolutional strategies, the introduction of separable convolutions for optimization, a unique fusion strategy, and a balanced tradeoff between performance and parameters. We believe that these features make our method competitive for structural damage detection and hold promise for effective real-world applications.

IV. Results Verification and Discussion

This section introduces the verification of the experimental results and discusses them. It also examines the changes in sensor performance before and after using the signal difference. Finally, it provides a comprehensive discussion and detailed comparison of our results with those in the relevant literature.

A. Detection Results Analysis

Table IV presents the results of the structural damage detection in each region using the signal difference and FCNND models. The trained model achieved accuracies ranging from 92.63% to 98.61% on the validation dataset and from 93.81% to 98.92% on the test dataset. Table IV shows that, except for zone 3rd with slightly lower predictive accuracy (93.81%), the detection accuracy in all other regions was above 98.20%. This demonstrates the outstanding performance of the enhanced sensor optimization for structural damage detection via a novel deep learning approach.

We analyzed this group using two graphical representations: 1) a confusion matrix, which provides insights into evaluating the model's performance and observing its misclassifications for different categories, and 2) a radar chart, which demonstrates each category's performance across different variables, facilitating comparisons and analyses of interclass variations. These two figures comprehensively illustrate our model's predictive performance across 11 categories under the worst case scenario, allowing us to gain a comprehensive understanding of the model's performance across different categories and features without revealing any significant instances of poor predictions. The detection performance of the FCNND3 model fell short of achieving an accuracy of the remaining detection zones (above 98%). By analyzing the confusion matrix and radar charts of the detection results in Fig. 10(a) and (b), we observed that sensors 29 and 30 exhibited more prediction errors and poorer feature representations during the detection process. In addition, we inferred from the performance evaluation of the distinguishable features and detection performance. The performance detection results of the sensor signals in Fig. 5 indicate that these two sensors also exhibited relatively lower performance in the undamaged/damaged binary classification. For FCNND3's ten sensors, there were three sensors in this zone with lower performance, which contributed to the inability to achieve more than 98% predictive performance in this zone.

B. Performance of Sensors With/Without Signal Difference

This section explores the reasons for this high predictive performance. This study focuses on enhanced sensor optimization for structural damage detection using a novel deep learning approach. An essential step in this approach is to assess the performance of the sensors following the concept of "having the right tools for the job." We selected five sensors out of the 30 sensors based on our previous findings from [31], which showed a relatively lower performance when the signal difference was not used. Including these sensors in the comparison allowed for a more in-depth analysis, and the results are presented in Table V.

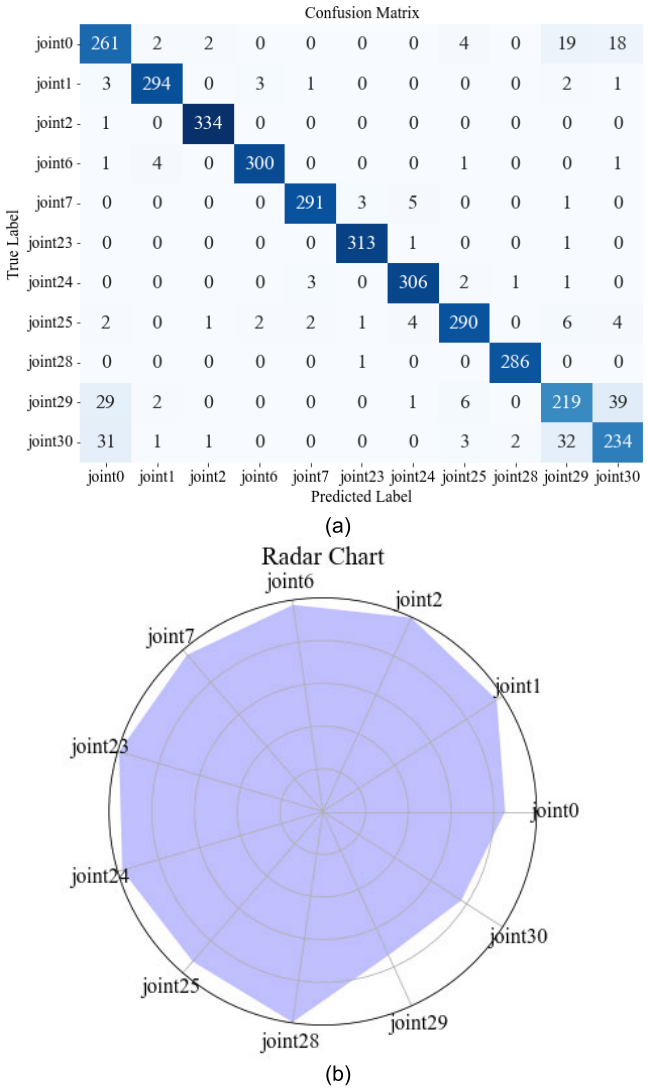

Fig. 10. Eleven-class prediction performance represented. (a) Eleven-class prediction performance represented by confusion matrix. (b) Eleven-class prediction performance represented by radar chart.

TABLE V
Binary Classification Accuracy: Sensors With/Without Signal Difference (Top 5 Poor Performing Sensors)

Sensor	Accuracy without Signal Difference	Accuracy with Signal Difference
	Kuo & Lee [31]	*The proposed method*
Sensor2	62.44%	94.63%
Sensor 10	83.42%	97.88%
Sensor 19	88.29%	94.63%
Sensor 29	62.11%	95.11%
Sensor 30	74.31%	96.25%

From Table V, it is evident that using the signal difference to replace the original joint vibration signals significantly enhances the sensor performance. Consequently, the model can effectively extract more vibration features.

C. Optimal Number of Sensors Evaluation

In accordance with the research conducted in [31], we adopted the metrics RS_{dr} and RS_{opt} as indicators. The structure under consideration features n joints, as shown in Fig. 3, where S_n denotes the aggregate number of sensors spanning the entire structure. Correspondingly, S_r signifies the minimal sensor count required for proficient damage detection in the structure, whereas S_{rmin} designates the least number of sensors for accurate detection. The evaluation of the sensor deployment efficacy is encapsulated by RS_{dr} and RS_{opt}, which represent the sensor demand rate and optimal sensor deployment, respectively. Quantification of the RS_{dr} results from applying

$$RS_{dr} = \frac{S_r}{S_n} \times 100\% \tag{10}$$

with RS_{opt} achieving zenith when RS_{dr} converges to its minimum threshold. The computation of RS_{opt} involves the interplay between S_{rmin}, S_n, and

$$RS_{opt} = \frac{S_{rmin}}{S_n} \times 100\%. \tag{11}$$

It is imperative to recognize that S_{dr} encapsulates the sensor requirements necessary for discerning structural damage, whereas S_{opt} is conceived from the standpoint of the optimal sensor quantity for discriminating between structurally damaged and undamaged states. Based on empirical experiments using the QUGS benchmark dataset, the observed values for S_r, S_n, and S_{rmin} were established as 30, 30, and 4, respectively. Consequently, the RS_{opt} value in this study was determined as 13.33%.

D. Discussion

Extensive research has been conducted on optimal sensor placement for structural damage detection, encompassing both traditional algorithms and deep learning methods. For instance, the GVPSS algorithm utilizes a geometric viewpoint for optimal sensor placement and parameter subset selection method [11]. They identified 14 sensors and specific installation locations as optimal for detecting damage in a 52-bar dome structure subjected to static and dynamic loading.

Similarly, Zhao et al. conducted a separate study employing the particle swarm optimization algorithm to explore the optimal sensor placement for 20 joints, ultimately determining that six sensors were optimal [37]. In a recent study, Blachowski et al. presented a comprehensive approach for damage identification in spatial truss structures, achieving remarkable results using only eight sensors placed at 23 joints [38]. In a recent study, Blachowski [38] presented a comprehensive approach for damage identification in spatial truss structures, achieving remarkable results using only eight sensors placed at 23 joints. Table VI compares the proposed method with the four cited references in terms of sensor quantity and placement. The results demonstrate that our method offers the advantages of minimal sensor usage and flexibility in terms of sensor location.

The literature collectively suggests that the optimal sensor placement and the number of sensors required for structural damage detection can vary based on the specific structure under analysis and the algorithm employed. Both traditional and deep learning approaches show promise for addressing this problem.

TABLE VI
SENSOR OPTIMIZATION COMPARISON

References	Sensor optimization results			
	Joints (Und./Dam.)	*Sensors*	*Sensor locations*	RS_{opt}
Beygzadeh et al. [11]	52	14	Ltd. locations	26.92%
Zhao et al. [37]	20	6	Ltd. locations	30%
Blachowski [38]	23	8	Ltd. locations	34.78%
Kuo & Lee [31]	30	5	Flex. sensor placement	16.67%
The proposed method	30	4	Flex. sensor placement	13.33%

Several deep learning algorithms have been proposed for structural damage detection. Abdeljabe et al. used a 1D-CNN model trained on the raw acceleration signals of 30 joints based on the QUGS dataset. Each CNN model evaluated whether a joint was damaged [15]. Ghazvinehwa et al. [17] used the same dataset to perform damage detection and localization on ten joints. Each joint trained a 2-D CNN model with three nearby acceleration data points and achieved 96.3%–96.3% accuracy on the test set. An accuracy of 97.4% was achieved.

Table VII compares the proposed method with the four cited references using deep learning approaches in terms of sensor utilization. The results demonstrate that our method offers the advantage of achieving a higher detection performance with fewer training models.

This study focused on statistical analysis and sensor optimization to enhance structural damage detection using deep learning. One of the challenges previously encountered was the inability of the models to extract features from sensor signals that are sufficient for conducting multiclass damage detection. Even with highly discerning sensors and selecting the most influential sensor combinations, caution is required during zone-based detection, as the presence of low-discrimination sensors can lead to significant variations in detection performance, resulting in accuracy levels as low as 80%. This problem has not been adequately addressed in the existing research, hindering effective breakthroughs in sensor optimization.

Regarding the methodology, we employed a signal difference approach in conjunction with fusion-based neural networks. Unlike methods that directly utilize vibration signals, the signal difference method replaces the vibration signals of damaged nodes and enables the discernment of subtle features in the sensor signals, leading to a substantial improvement in damaged/undamaged binary classification detection. Without using a signal difference, the sensor detection performance ranged from 62.11% to 98.70%. However, after applying the signal difference, the sensor detection per-

TABLE VII
COMPARISON OF SENSOR PLACEMENT AND MODEL PERFORMANCE FOR STRUCTURAL DAMAGE PREDICTION

	Optimal sensor locations and accuracy							
	Joints (Und./ Dam.)	*Models*	*Sen.*	Sensor locations	RS_{opt}	*Vali. Accuracy*	*Test Accuracy*	*adjustable parameters*
O.Abdeljaber et al. [15]	30	30 CNN	30	Ltd. locations	100%			lr: initial 0.001 lr_increase 5% lr_reduce 30% Epochs:100 Kernel size 41 Stride 2 Trial-and-error
S.Ghazvineh et al. [17]	10	10 CNN	10	Ltd. locations	100%	95.30% ~ 96.00%	96.30% ~ 97.40%	Activation: ReLU
Kuo & Lee [31]	30	4 CNN	5	Ltd. locations	16.60%	79.17% ~ 96.60%	80.39% ~ 96.62%	lr:0.001 Epochs:300 Batch size: 128 Opt. Algorithm: Adam Activation: ReLU Kernel size (50, 8, 3, 2) Pooling size (2, 8, 8, 8) L1=10^{-5} L2=10^{-4} Droup:0.5
The proposed method	30	5 FCNND	4	Flex. sensor placement	13.33%	92.63% ~ 98.73%	93.81% ~ 98.92%	lr:0.0005 Epochs:300 Batch size: 128 Opt. Algorithm: Adam Activation: ReLU Kernel size (100, 5, 3, 2) Pooling size (2, 8, 8, 8) L1=6×10^{-5} L2=8×10^{-4} Droup:0.7

formance significantly increased from 94.63% to 99.51%. Notably, the application of signal differences to sensor combinations demonstrated marked differences. In the absence of a signal difference, the selection of sensor combinations presents considerable challenges for zone-based detection. Conversely, using sensor combinations with a signal difference results in stability and reliability, facilitating more effective zoning for detection and solving the inconvenience of partition detection in zones. In addition, a potential advantage of the signal difference method is its ability to effectively reduce the impact of uncertainty on sensors. Furthermore, this study employed a fusion-based neural network model to handle signal differences and detect structural damage. This specialized neural network not only reduced the parameter count and improved the detection efficiency but also significantly enhanced the damage detection accuracy, outperforming conventional single-model approaches.

From the perspective of the data and experimental results, the previous approach achieved detection performances ranging from 80.39% to 96.62%. In contrast, our present study demonstrated a predictive performance between 93.81% and 98.92%, markedly increasing the accuracy. These results strongly confirm the effectiveness of the proposed method. Our proposed method yielded meaningful and valuable outcomes, featuring diversity and versatility in sensor location selection, and demonstrated optimization advantages in terms of sensor quantity. These results contribute to resolving the current challenges in sensor detection and promote advancements in relevant fields.

Our signal difference approach involves subtracting the vibration signals obtained from the damaged and securely fastened undamaged states. In the securely fastened, undamaged state, the structural components are tightly secured by controlled tightening using torque wrenches or controlled bolts, thereby ensuring a stable and unchanging reference state for the undamaged vibration signal. Consequently, at any given time point, a signal difference analysis can be effectively conducted by subtracting the vibration signal associated with structural damage from the reference undamaged vibration signal.

The signal difference method has demonstrated remarkable efficacy in extracting subtle features indicative of structural damage, thereby significantly enhancing the effectiveness of structural damage detection. By utilizing the securely fastened undamaged vibration signal as a stable reference, signal difference analysis facilitates the discernment of distinct damage-related characteristics in the vibration signals captured at different time points.

It is important to ensure that the vibration signals used for the signal difference analysis are sampled at the same frequency and have identical data lengths. This consideration is essential to ensure accurate and reliable computations during the signal differencing process and to maintain the consistency of the reference undamaged vibration signal.

Furthermore, signal difference analysis can be complemented by leveraging advanced feature extraction techniques and deep learning methodologies. This integrated approach allows for a comprehensive and sophisticated analysis of the extracted features, potentially yielding even more robust and accurate structural damage detection outcomes.

In summary, our signal difference method, wherein the damaged vibration signal is replaced with the difference between the damaged and securely fastened undamaged vibration signals, enhances the structural damage detection capabilities. By utilizing a securely fastened undamaged vibration signal as a reference, this method enables the extraction of meaningful damage-related features and contributes significantly to the advancement of SHM methodologies.

In this study, we employed an enhanced structural damage identification (SDI) approach that addresses sensor identifiability, detection zones, and sensor optimization, as discussed in the literature. However, the effectiveness of our detection method was influenced by several factors. First, despite our optimization efforts, sensor identifiability remains a challenge in real-world deployment and calibration. Future research can further advance the sensor technology to improve identifiability and responsiveness. Second, the quality of the vibration signals significantly affected the detection outcomes. Although

we implemented signal replacement techniques, there is room for further improvement. Subsequent studies can focus on enhancing the signal quality. Finally, the data collection process is crucial. However, practical scenarios may introduce data quality and completeness issues. Future research should explore efficient and reliable data collection methods to ensure accurate structure detection. In summary, our study represents a significant improvement in addressing the key issues in SDI. Nevertheless, we recognize the ongoing challenges and encourage future researchers to enhance the accuracy and reliability of structural detection.

V. Conclusion

In this study, we propose an innovative method that uses deep learning techniques to detect damage in plane steel frame structures. By replacing the signal of the damaged nodes with the signal difference between the damaged and undamaged nodes, we analyzed all sensors using statistical methods. The sensor performance was evaluated based on the mean, standard deviation, and scatter plot of the sensor prediction performance, thereby achieving robustness in sensor combinations. This method not only facilitates sensor selection but also provides robustness in the sensor combination compared to previous research, offering significant flexibility in planning detection zones. The detection performance improved significantly from 93.81% to 98.92%, demonstrating its effectiveness in mitigating the influence of uncertain environmental factors.

To construct an accurate and efficient damage detection model, we employed a 1D-FCNND with multiple convolutional layers. The practical application of our method was successfully validated using benchmark data from QUGS. The results demonstrated a remarkable reduction in sensor demand, requiring only 13.33% of the total number of sensors while significantly improving the damage detection accuracy (98.92%) using only five 1D-FCNND models. Our approach offers significant advantages in terms of simplicity and robustness, leading to an enhanced detection performance and optimized sensor utilization. It was demonstrated as a viable and efficient solution for SHM and damage detection in plane steel frame engineering. By streamlining the sensor selection and improving the detection efficiency, our method shows practical value in advancing the field of SHM and damage detection.

References

[1] L. Song, S. Li, J. Wang, Z. Wang, and G. Zhao, "Research progress on structural damage identification in civil engineering," in *Proc. Int. Conf. Intell. Transp., Big Data Smart City (ICITBS)*, Jan. 2020, pp. 337–344, doi: 10.1109/ICITBS49701.2020.00076.

[2] L.-T. Zhang, "Effect of damping coefficients on structural damage identification," in *Proc. IEEE 10th Joint Int. Inf. Technol. Artif. Intell. Conf. (ITAIC)*, vol. 10, Jun. 2022, pp. 123–127, doi: 10.1109/ITAIC54216.2022.9836535.

[3] S. Sun, C. Liao, A. M. Hafez, H. Zhu, and S. Wu, "Two-dimensional MXenes for energy storage," *Chem. Eng. J.*, vol. 338, pp. 27–45, Apr. 2018, doi: 10.1016/j.cej.2017.12.155.

[4] A. K. Pandey, M. Biswas, and M. M. Samman, "Damage detection from changes in curvature mode shapes," *J. Sound Vib.*, vol. 145, no. 2, pp. 321–332, 1991, doi: 10.1016/0022-460X(91)90595-B.

[5] O. S. Salawu, "Detection of structural damage through changes in frequency: A review," *Eng. Struct.*, vol. 19, no. 9, pp. 718–723, Sep. 1997, doi: 10.1016/S0141-0296(96)00149-6.

[6] P. Reynolds, A. Pavic, and Z. Ibrahim, "A remote monitoring system for stadia dynamics," *Proc. Inst. Civil Eng.-Struct. Buildings*, vol. 157, no. 6, pp. 385–393, Dec. 2004, doi: 10.1680/stbu.2004.157.6.385.

[7] S. W. Doebling et al., "Damage identification and health monitoring of structural and mechanical systems from changes in their vibration characteristics: A literature review," Shock Vib. Dig., 30, Tech. Rep. LA-13070-MS, Los Alamos Nat. Lab., Los Alamos, NM, USA, May 1996, doi: 10.2172/249299.

[8] F. Magalhães, A. Cunha, and E. Caetano, "Vibration based structural health monitoring of an arch bridge: From automated OMA to damage detection," *Mech. Syst. Signal Process.*, vol. 28, pp. 212–228, Apr. 2012, doi: 10.1016/j.ymssp.2011.06.011.

[9] M. L. Fugate, H. Sohn, and C. R. Farrar, "Vibration-based damage detection using statistical process control," *Mech. Syst. Signal Process.*, vol. 15, no. 4, pp. 707–721, Jul. 2001, doi: 10.1006/mssp.2000.1323.

[10] S. Beygzadeh, E. Salajegheh, P. Torkzadeh, J. Salajegheh, and S. S. Naseralavi, "An improved genetic algorithm for optimal sensor placement in space structures damage detection," *Int. J. Space Struct.*, vol. 29, no. 3, pp. 121–136, Sep. 2014, doi: 10.1260/0266-3511.29.3.121.

[11] S. Beygzadeh, P. Torkzadeh, and E. Salajegheh, "Optimal number and location of sensors for structural damage detection using the theory of geometrical viewpoint and parameter subset selection method," *Periodica Polytechnica Civil Eng.*, vol. 66, no. 3, pp. 809–819, 2022, doi: 10.3311/ppci.19695.

[12] T.-H. Yi, H.-N. Li, and M. Gu, "Optimal sensor placement for health monitoring of high-rise structure based on genetic algorithm," *Math. Problems Eng.*, vol. 2011, pp. 1–12, May 2011, doi: 10.1155/2011/395101.

[13] Y. Yu, C. Wang, X. Gu, and J. Li, "A novel deep learning-based method for damage identification of smart building structures," *Struct. Health Monitor.*, vol. 18, no. 1, pp. 143–163, Jan. 2019, doi: 10.1177/1475921718804132.

[14] H. Khodabandehlou, G. Pekcan, and M. S. Fadali, "Vibration-based structural condition assessment using convolution neural networks," *Struct. Control Health Monit.*, vol. 26, p. e2308, Feb. 2019, doi: 10.1002/stc.2308.

[15] O. Abdeljaber, O. Avci, S. Kiranyaz, M. Gabbouj, and D. J. Inman, "Real-time vibration-based structural damage detection using one-dimensional convolutional neural networks," *J. Sound Vibrat.*, vol. 388, pp. 154–170, Feb. 2017, doi: 10.1016/j.jsv.2016.10.043.

[16] O. Abdeljaber. (2019). *Structural Damage Detection (Public Website)*. [Online]. Available: http://www.structuraldamagedetection.com/

[17] S. Ghazvineh, G. Nouri, S. H. H. Lavassani, V. Gharehbaghi, and A. Nguyen, "Application of 2-D convolutional neural networks for damage detection in steel frame structures," 2021, *arXiv:2110.15895*.

[18] Z. Teng, S. Teng, J. Zhang, G. Chen, and F. Cui, "Structural damage detection based on real-time vibration signal and convolutional neural network," *Appl. Sci.*, vol. 10, no. 14, p. 4720, Jul. 2020, doi: 10.3390/app10144720.

[19] K. Tao, T. Liu, Q. Wang, H. Wang, Y. Cheng, and D. Yue, "A structural monitoring data processing model based on signal musicalization," *Measurement*, vol. 199, Aug. 2022, Art. no. 111563, doi: 10.1016/j.measurement.2022.111563.

[20] R. Ravindran, M. J. Santora, and M. M. Jamali, "Camera, LiDAR, and radar sensor fusion based on Bayesian neural network (CLR-BNN)," *IEEE Sensors J.*, vol. 22, no. 7, pp. 6964–6974, Apr. 2022.

[21] E. L. Chuma and T. Rasmussen, "Metamaterial-based sensor integrating microwave dielectric and near-infrared spectroscopy techniques for substance evaluation," *IEEE Sensors J.*, vol. 22, no. 20, pp. 19308–19314, Oct. 2022.

[22] K. Haneda, K. Matsudaira, and H. Takahashi, "Neural network-based airflow vector sensor using multiple MEMS differential pressure sensors," *IEEE Access*, vol. 11, pp. 40978–40987, 2023.

[23] P. Ong, Y. K. Tan, K. H. Lai, and C. K. Sia, "A deep convolutional neural network for vibration-based health-monitoring of rotating machinery," *Decis. Anal. J.*, vol. 7, Jun. 2023, Art. no. 100219, doi: 10.1016/j.dajour.2023.100219.

[24] (Jun. 2021). *A New Experimental Benchmark Problem for Vibration-Based Structural Health Monitoring (SHM) Structural Dynamics Team*. [Online]. Available: http://www.structuralvibration.com/benchmark/

[25] A. Garofalo, N. Testoni, A. Marzani, and L. De Marchi, "Wavelet-based Lamb waves direction of arrival estimation in passive monitoring techniques," in *Proc. IEEE Int. Ultrason. Symp. (IUS)*, Sep. 2016, pp. 1–4, doi: 10.1109/ULTSYM.2016.7728808.

[26] P. Hu, H. Wang, G. Tian, Z. Dong, F. Qiu, and B. F. Spencer, "Wireless localization of spallings in switch-rails with guided waves based on a time-frequency method," *IEEE Sensors J.*, vol. 19, no. 23, pp. 11050–11062, Dec. 2019, doi: 10.1109/JSEN.2019.2934159.

[27] F. Chollet, "Xception: Deep learning with depthwise separable convolutions," in *Proc. IEEE Conf. Comput. Vis. Pattern Recognit. (CVPR)*, Jul. 2017, pp. 1800–1807, doi: 10.1109/CVPR.2017.195.

[28] A. G. Howard et al., "MobileNets: Efficient convolutional neural networks for mobile vision applications," 2017, *arXiv:1704.04861*.

[29] A. Howard et al., "Searching for MobileNetV3," in *Proc. IEEE/CVF Int. Conf. Comput. Vis. (ICCV)*, Oct. 2019, pp. 1314–1324.

[30] Y. Liang, Y. Zhou, T. Wan, and X. Shu, "Deep neural networks with depthwise separable convolution for music genre classification," in *Proc. IEEE 2nd Int. Conf. Inf. Commun. Signal Process. (ICICSP)*, Weihai, China, Sep. 2019, pp. 267–270, doi: 10.1109/ICICSP48821.2019.8958603.

[31] C.-C. Kuo and C.-H. Lee, "Optimization of sensors for structure damage detection using deep learning approach," *IEEE Sensors J.*, vol. 23, no. 21, pp. 26401–26410, Aug. 2023, doi: 10.1109/JSEN.2023.3301171.

[32] K. C. Chao, Y. Shih, and C. H. Lee, "A novel sensor-based label-smoothing technique for machine state degradation," *IEEE Sensors J.*, vol. 23, no. 10, pp. 10879–10888, May 2023, doi: 10.1109/JSEN.2023.3263634.

[33] P. M. Huang and C. H. Lee, "Estimation of tool wear and surface roughness development using deep learning and sensors fusion," *Sensors*, vol. 21, no. 16, p. 5338, 2021, doi: 10.3390/s21165338.

[34] Y. Lecun et al., "Gradient-based learning applied to document recognition," *Proc. IEEE*, vol. 86, no. 11, pp. 2278–2324, Nov. 1998, doi: 10.1109/5.726791.

[35] D. Jung et al., "Sensor selection for fault diagnosis in uncertain systems," *Int. J. Control*, vol. 92, no. 11, pp. 2509–2522, Jun. 2018, doi: 10.1080/00207179.2018.1484171.

[36] R. Suchy, S. Ezekiel, and M. Cornacchia, "Fusion of deep convolutional neural networks," in *Proc. IEEE Appl. Imag. Pattern Recognit. Workshop (AIPR)*, Sep. 2018, doi: 10.1109/AIPR.2017.8457945.

[37] J. Zhao et al., "Optimal sensor placement for a truss structure using particle swarm optimisation algorithm," *Int. J. Acoust. Vib.*, vol. 22, no. 4, pp. 439–447, Dec. 2017, doi: 10.20855/ijav.2017.22.4489.

[38] B. Blachowski, "Modal sensitivity based sensor placement for damage identification under sparsity constraint," *Periodica Polytechnica Civil Eng.*, vol. 63, pp. 432–445, 2019. [Online]. Available: https://pp.bme.hu/ci/article/view/13888

Chien-Chih Kuo received the M.S. degree in civil engineering from Chung Yuan Christian University, Taoyuan City, Taiwan, in 1997. He is currently pursuing the Ph.D. degree with the Institute of Electrical and Control Engineering, National Yang Ming Chiao Tung University, Hsinchu, Taiwan.

His research interests include the Internet of Things and AI applications.

Dr. Kuo is currently a Professional Civil Engineer and a Taoyuan City Building Construction Committee Member and TPCE of Earthquake Resistance Certification Committee Member.

Ching-Hung Lee (Senior Member, IEEE) was born in Taiwan, in 1969. He received the B.S. and M.S. degrees from the Department of Control Engineering, National Chiao Tung University, Hsinchu, Taiwan, in 1992 and 1994, respectively, and the Ph.D. degree from the Department of Electrical and Control Engineering, National Chiao Tung University, in 2000.

He is currently a Distinguished Professor with the Institute of Electrical and Control Engineering, National Yang Ming Chiao Tung University, Hsinchu. His research interests include artificial intelligence, smart manufacturing, fuzzy neural systems, signal processing, nonlinear control systems, robotics control, and CNC motion control and optimization.

Dr. Lee received the Researcher Excellent Award and Wu Ta-Yu Medal (Young Researcher Award) from the National Science and Technology Council, Taiwan, in 2023 and 2008, respectively. He was also awarded the Fellow, Youth, and Excellent Automatic Control Engineering Awards from the Chinese Automatic Control Society, Taiwan, in 2019, 2009, and 2016, respectively.